Discrete Element Analysis of Idealized Granular Geometric Packings Subjected to Gravity

Michael A. Faraone[1], Jae H. Chung*[1], Michael T. Davidson[1]

[1]Bridge Software Institute, University of Florida, P.O. Box 116580, Gainesville, Florida, 32611, United States

*Corresponding author: JCHUN@CE.UFL.EDU

1 Introduction

This paper presents discrete element analysis models for studying quasi-static stress states in idealized granular materials subjected to gravity, and utilizes geometric packings and contact mechanics. The theoretical description of granular materials in assemblies of microscopic particles is a challenging task. The particle assemblies characterize in-situ initial and boundary conditions. In turn, the conditions are used in solving the equations of motion of the particulate system under stress equilibrium states (via a network of particle contact forces and various degrees of dissipative interparticle friction). Using the discrete element analysis model of LS-DYNA [1], the influence of packing on contact stress distributions within an explicit time domain is investigated using idealized assemblies of spherical discrete elements and contact penalty springs. The validity of idealized geometric packings, as to whether uniformity can simulate granular fabrics, is still a matter of debate. However, the present study strictly focuses on the effects of micromechanical structures (idealized by assemblies of spherical discrete elements) in stress states at a macroscopic scale. In this context, the macroscopic scale is associated with the size of samples used for direct shear experiments in laboratory settings).

Modeling of in-situ conditions in geotechnical engineering problems requires simulation of a geostress state known as the "at rest" condition, where stress equilibrium states of granular masses under gravitational body forces vary in phenomenological observations [2]. As a result, force propagations that arise due to externally applied forces are affected by these non-zero stress states. Phenomenologically, this is described by the ratio of horizontal, σ_h, to vertical stress, σ_v:

$$K_o = \frac{\sigma_h}{\sigma_v} = 1 - \sin \varphi \qquad (1)$$

where the ratio is termed the coefficient of earth pressure at rest, K_o. Note that K_o is defined as a function of the macroscopic characteristics, i.e., the angle of internal friction φ [3]. Alternatively stated, the macroscopic kinematics of a control volume of the granular masses is the controlling phenomenological factor of the geostress equilibrium state at rest. This study is focused on various geometric packings (with uniquely characteristic coordination numbers) as a means of simulating geostatic equilibrium states through use of the discrete element method. The simulation results are discussed regarding selected modeling parameters. Cataloged coordination numbers, considered along with a set of discrete contact properties (interparticle frictional coefficients), are used in a parametric sensitivity study aimed at simulating the effects of granule-to-granule interlocking in the macroscopic characteristics. Macroscopic shear strengths, which vary per packing assembly, are investigated through use of a parametric matrix of direct shear test simulations. Based on the Biot theory and numerical results obtained from constrained chmaber test simulations, averaged stresses over a control volume of the assemblies are studied to qualitatively correlate macroscopic shear strengths of packing assemblies with existing semi-empirical methods.

2 Geometric Packing

The four packing assemblies used for this work are shown in Fig. 1, where the gray circles represent an individual row of spheres and the black circles represent the arrangement of spheres on the level above the gray set. These figures represent the unit cell for the packing, or the basic structure that repeats itself throughout the assembly. The first two sets of packing assemblies shown in Fig. 1 are the face centered cubic (FCC) and Rhombic (also referred to as tetrahedral or hexagonal close

packing). These two packing arrangements are theoretically considered to be the densest arrangement for uniformly sized spheres.

The third and fourth packing assemblies shown in Fig. 1 are referred to as binary packing structures since two different sets of radii are present. The first binary packing developed is called the simple cubic binary, which is based on the simple cubic packing structure with the addition of smaller spheres (with radius R_{min}) located within the available space between layers of the larger sphere set (R_{max}).

The second binary packing structure is referred to as the AB Binary. This packing was developed using the cubical-tetrahedral packing structure with the addition of smaller spheres located within the available space between layers of larger spheres. Summaries of the geometric packing assemblies are listed in Table 1. The coordination number is defined as the average number of contacts per sphere. It can be seen that the addition of a smaller sphere set increases the density of packing (corresponds to a smaller void ratio), but the coordination numbers of such binary packings are less than 12 as the limiting coordination number.
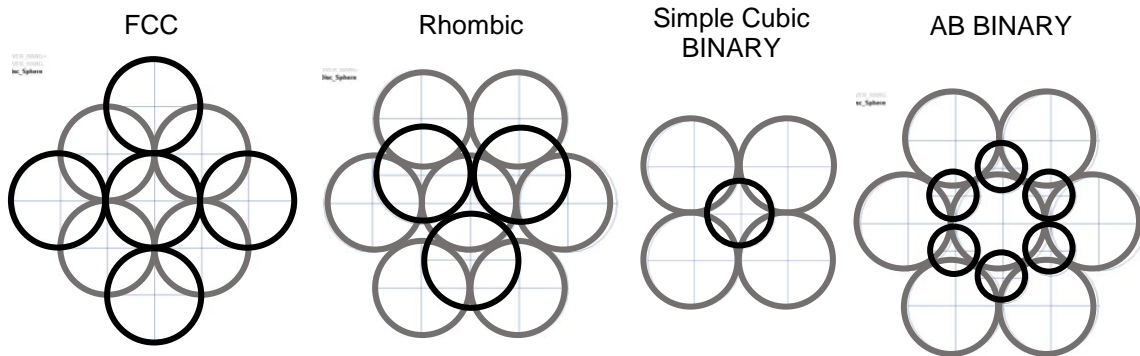

Fig.1: Geometric Packing Assemblies

Type of Packing	Coordination Number	Layer Spacing	Porosity [%]	Void Ratio	R_{min}/R_{max}
FCC	12	$\sqrt{2}R$	25.95	0.35	1
Rhombic	12	$2\sqrt{2/3}R$	25.95	0.35	1
Simple Cubic BINARY	11.1	$2R$	23.83	0.31	$\sqrt{3}-1$
AB BINARY	10.7	$2R$	22.65	0.29	$\sqrt{7/3}-1$

Table 1: Properties of Geometric Packings for use in LS-DYNA Discrete Element Analysis: Layer spacing for binary packing based on R_{max}

In the present study of macroscopic-scale shear behaviors of idealized packings, discrete element analysis models are developed using LS-DYNA. The motion of each sphere is computed using Newton's laws of motion, allowing for both translations and rotations at the centroid. Interactions between spheres are controlled through specification of frictional coefficients, along with spring and damping constants, which are defined in both normal and tangential directions to the plane of spherical surface contact [4]. A penalty-spring method is used by defining the ***CONTROL_DISCRETE_ELEMENT** card. Material properties such as mass density and bulk moduli are defined using material definition cards (e.g., ***MAT_ELASTIC**). Note that capillary forces were not utilized in the current study; a summary of the DEM input parameters used in this study are listed in Table 2. Three values of FRIC, the interparticle sliding friction coefficient (0.1, 0.3 and 0.5), are used in a parametric study to develop a range of φ values in conjunction with the aforementioned packing structures. Normal and tangential damping parameters, NDAMP and TDAMP respectively, are used to ensure numerical stability and are recommended values from Karajan [4]. The focus of this work is placed solely on the effects that the packing assemblies and FRIC values have on macroscopic φ behavior, thus the frictional rolling coefficient FRICR is set to zero. The normal-contact spring scale factor, NORMK, is set 1 and the ratio of tangential to normal stiffness, SHEARK, is set to 0.5 as used by Cil [5]. Mass density and modulus values are selected to prevent significant particle overlapping for

the magnitudes of pressure imposed during the direct shear and chamber tests, while also promoting practical computational times.

LS-DYNA Discrete Element Analysis Parameter	Value
Radius	5 mm
NDAMP	0.70
TDAMP	0.40
FRIC	0.1, 0.3, 0.5
FRICR	0
NORMK	1.0
SHEARK	0.5
Mass Density	3,000 kg/m^3
Elastic Modulus	300 MPa
Poisson's Ratio	0.33333

Table 2: Input Parameters of LS-DYNA Discrete Element Analysis

3 Simulations of Direct Shear Test

Direct shear tests (DST) are simulated to quantitatively characterize the macroscopic shear behaviors of the packings. The model shown in Fig. 2a is comprised of a box that houses the discrete elements. This box is divided in half horizontally; the upper half is laterally displaced according to a prescribed displacement boundary condition, while the lower half is held fixed. The top plate allows for the application of a constant normal pressure during shearing. Two overhanging plates are positioned in front and behind the direction of shearing to prevent discrete elements from escaping.
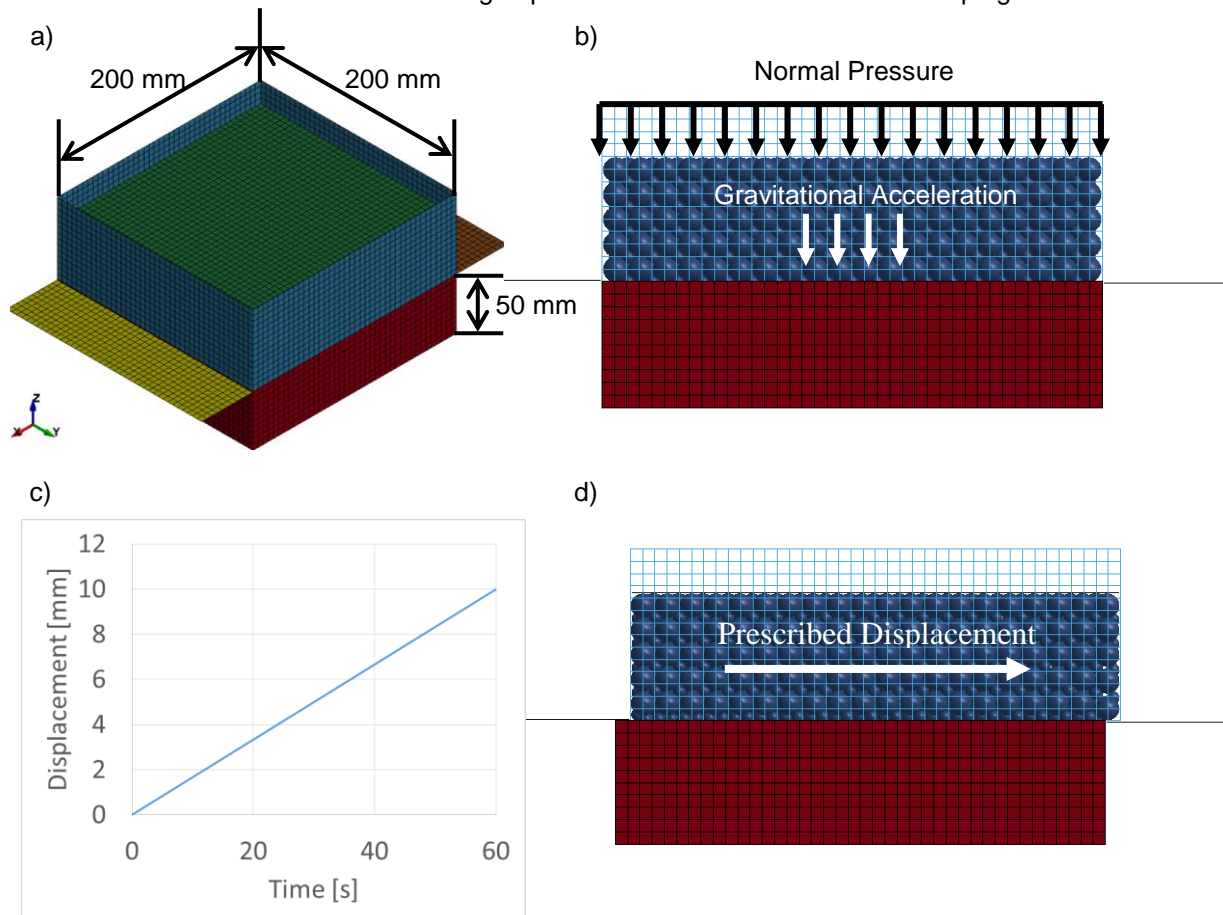

Fig.2: Direct Shear Test: a) Isometric View b) Applied Pressure and Gravitational Acceleration c) Prescribed Displacement Curve d) Prescribed Displacement.

3.1 Direct Shear Analysis Model

The walls of the DST model consist of fully-integrated four-node shell elements, which are paired with the ***MAT_RIGID** material model. Constitutive parameters used to populate the ***MAT_RIGID** card are set equal to those of the discrete elements listed in Table 2. Shown in Fig. 2b are the applied pressure to the top plate and gravitational acceleration (9.81 m/s^2) is applied to the discrete spheres. All excitations are applied quasi-statically by making use of the ***CONTROL_DYNAMIC_RELAXATION** card. Boundary conditions for the shell elements are specified using constraint options available with the ***MAT_RIGID** card. The bottom box and front overhanging plate have all degrees of freedom restrained from motion. The top box, top plate, and back overhang plate are free to translate in the direction of shearing, in this case the X-direction, and are restrained from motion in the Y direction. For the top box, top plate, and back overhang plate, X-direction motion is prescribed for a total distance of 10 mm over 60 seconds of simulation time (Fig. 2c-d). The top box and back overhang plate are restrained from vertical (Z) motion, whereas the top plate is permitted to translate vertically to allow for vertical displacements of the discrete element mesh.

The DST apparatus (Fig, 2a) is 200 mm in width by 100 mm in height. Each packing assembly can have a different sized unit cell for the same specified radius, thus not all packing assemblies can fill the respective, specified domains without gaps developing between spheres and the DST walls.

Any gaps between arrays of spheres and the walls of the DST apparatus are not ideal. When initial gaps are present, application of gravitational accelerations or applied normal stress may cause significant rearrangement of the sphere arrays due to absence of lateral confinement. To account for such gaps, the DST dimensions in both the X and Y directions are scaled so as to encase the assembly, (i.e., initial gaps are approximately equal to 0 mm). Contact between the discrete spheres and shell elements is specified using the ***CONTACT_AUTOMATIC_NODES_TO_SURFACE** card. The coefficient of sliding friction used in the shell-spheres contact is set equal to FRIC (Table 2).

3.2 Estimation of Angles of Internal Friction

To estimate the frictional resistance of the packing, normal stresses are applied, and the corresponding maximum shear stresses are plotted. Shear stresses on the samples are calculated by first measuring lateral forces (in the direction of shearing) acting on the top box and plate. These forces are recorded using the ***DATABASE_RCFORCE** card and are divided by the cross sectional area of the sample. An example of this process begins with Fig. 3a, which is shear stress versus shear strain for testing of the Rhombic packing assembly, FRIC = 0.3, and normal stresses of 50, 100 and 150 kPa. Peak shear stress values are found for each normal stress and are summarized in Table 3. These pairs of points are then plotted in Fig. 3b, for which a regression line can be fitted using a least-squares approximation. The angles of internal friction (φ) are determined per the slope of the fitted line. For the Rhombic packing example, using the fitted line from Fig. 4: $\varphi = \tan^{-1}(1.1535) = 49.1°$.
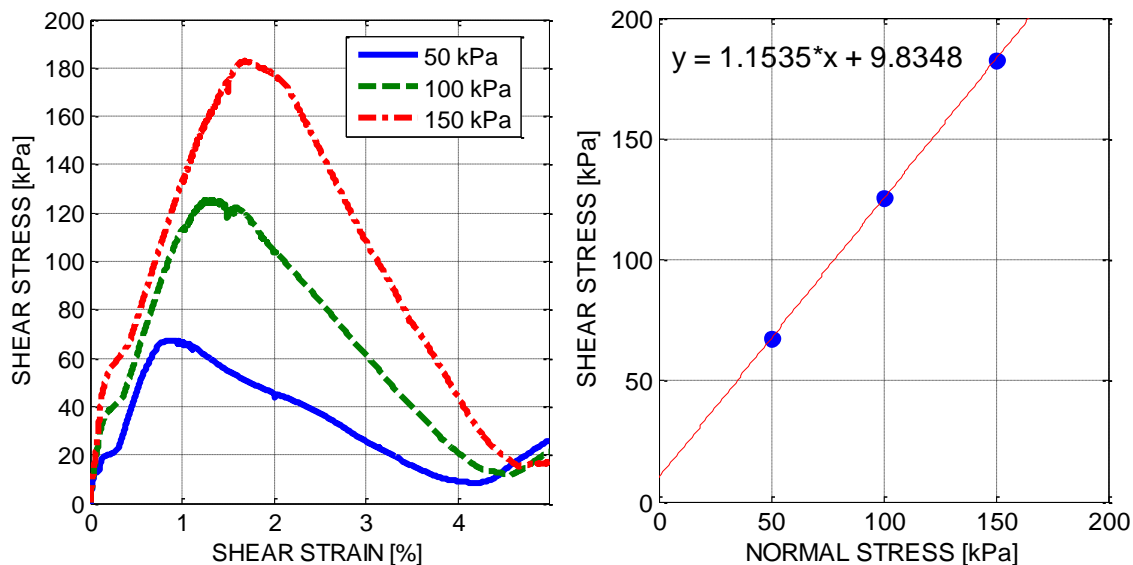

Fig.3: Direct Shear Test Results: Rhombic FRIC =0.3 Normal Stress = 50, 100, and 150 kPa. a) Shear Stress versus Shear Strain b) Shear Stress versus Normal Stress

Normal Stress [kPa]	Peak Shear Stress [kPa]	Void Ratio Before Shearing
50	67.3	0.433
100	125.4	0.431
150	182.7	0.429

Table 3: Stresses Averaged over Failure Plane

3.3 Parametric Simulation Results

Results from the parametric study for various combinations of packing assemblies and coefficients of friction are shown in Fig. 4. For the rhombic and FCC packing, there is a relationship between coefficient of friction and φ. For the binary packing assemblies, a relationship is not as readily apparent (φ does not increase as significantly for increasing values of FRIC).
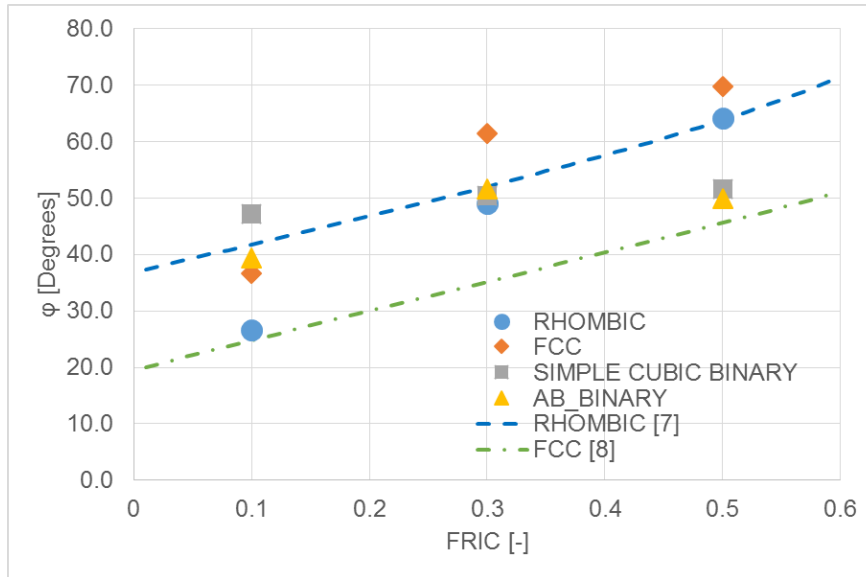

Fig.4: Parametric Results from Direct Shear Test.

It is also observed that φ for the FCC packing is greater than that of the Rhombic packing. As reported by O'Sullivan [6], for two physical triaxial compression tests of 12.7 mm diameter steel spheres, φ values of 41.6° and 24.6° were measured for Rhombic and FCC packings, respectively. O'Sullivan [6] also reported comparable results for DEM modeling of the triaxial compression tests using a FRIC value of 0.096, resulting in φ values of 42° and 23.5° for Rhombic and FCC packings, respectively. Additionally, theoretical expressions to estimate the peak strength of Rhombic packings (Rowe [7]) and FCC packings (Thorton [8]) show agreement in that for any value of interparticle friction, the Rhombic packing will have a higher peak strength than that of the FCC packing. These theoretical expressions are shown in Eqns. 2 and 3 for Rhombic [7] and FCC [8] packings, respectively.

$$\frac{\sigma_1}{\sigma_3} = \frac{\left(4 + 2\sqrt{2}\,FRIC\right)}{\left(1 - \sqrt{2}\,FRIC\right)} \tag{2}$$

$$\frac{\sigma_1}{\sigma_3} = \frac{2\left(1 + FRIC\right)}{\left(1 - FRIC\right)} \tag{3}$$

where σ_1 is the major principle stress and σ_3 is the minor principle stress. Using Eqn. 4, φ can be evaluated using principal stresses, and can be combined with Eqns 2-3, to evaluate φ as a function of FRIC (recall Table 1):

$$\varphi = \sin^{-1}\left[\frac{\left(\sigma_1 - \sigma_3\right)}{\left(\sigma_1 + \sigma_3\right)}\right] \tag{4}$$

Results of this combination are shown in Fig. 4 as dashed lines. Validation of the previously discussed DST apparatus was carried out by comparing results from numerical direct shear tests to results reported in O'Sullivan [9]. The validation consisted of modeling steel spheres arranged in a random packing. The DST, as modeled in the current study, produced a φ of 21.1°, where over the course of repeated testing, O'Sullivan [9] measured φ values ranging from 22.7° to 26.2°. The comparable benchmarking results (for randomly distributed spheres) suggest that geometrical arrangement of the packing assemblies may lead to significant differences in φ values observed in triaxial versus direct shear testing. Future research is needed to explore such differences.

4 Scale-Dependent Stress States

To evaluate the stress state of each geometric assembly, a chamber test is conducted. The chamber test is shown in Fig. 5a, and has dimensions of 500x500x1000 mm. Lateral confinement for the chamber is provided by constraining the degrees of freedom of the spheres initially positioned nearest to the boundary of the chamber, Fig. 5b. Spheres located on the bottom of the chamber have all degrees of freedom (translations and rotations) restrained. Spheres located on the edge of the chamber are only permitted to translate in the vertical (Z) direction. Gravitational acceleration (9.81 m/s²) is applied to the discrete elements quasi-statically through use of the ***CONTROL_DYNAMIC_RELAXATION** card. After the assembly reaches a quasi-static force equilibrium state, stresses in both the horizontal direction and vertical direction are cataloged. The cataloged stresses constitute average stresses for individual spherical volumes of the discrete elements, σ_{ij}^{local} [10]:

$$\sigma_{ij}^{local} = \frac{\sum_{i=1}^{n_c} f_i \otimes b_j}{V_{sphere}}$$

(5)

where n_c is the number of contacts, f is the vectorial contact force, b is the branch vector from the centroid to the point of contact, and V_{sphere} is the sphere volume. An example of results for σ^{local} in the Z direction are shown in Fig. 6a for the chamber test (using Simple Cubic Binary Packing and a FRIC value of 0.3). As shown, the stress profile increases linearly with depth and is constant in the horizontal direction. Note that it was verified that lateral confinement provided by the constrained spheres does not have a significant impact on the resulting sphere stresses near the chamber boundaries.

Importantly, computations of σ_v and σ_h across the range of packings considered necessitate the definition of a control volume, which in turn, determines volume-averaged shear resistance, i.e., the value of φ (recall Fig. 2). Over a control volume V_{cv}, the averaged stress, σ^{total}, is calculated as:

$$\sigma^{total} = \frac{V_{cv} - V_s}{V_{cv}} \left(\sum_{n_p} \sigma^{local} \right)$$

(6)

which n_p denotes the number of discrete elements within V_{cv} and V_s is the volume of solid phase; $V_s = n_p \cdot V_{sphere}$. Thus, macroscopic stresses estimated using Eqn. 6 depend on the size of the control volume per continuum-based approaches. For Simple Cubic Packing (with a FRIC value of 0.3), the profiles of σ_v and σ_h (calculated using Eqn. 6) are shown in Fig. 6b and the corresponding K_o is plotted in Fig. 6c. Both σ_v and σ_h profiles increase linearly with depth. In turn, K_o remains constant throughout the depth.
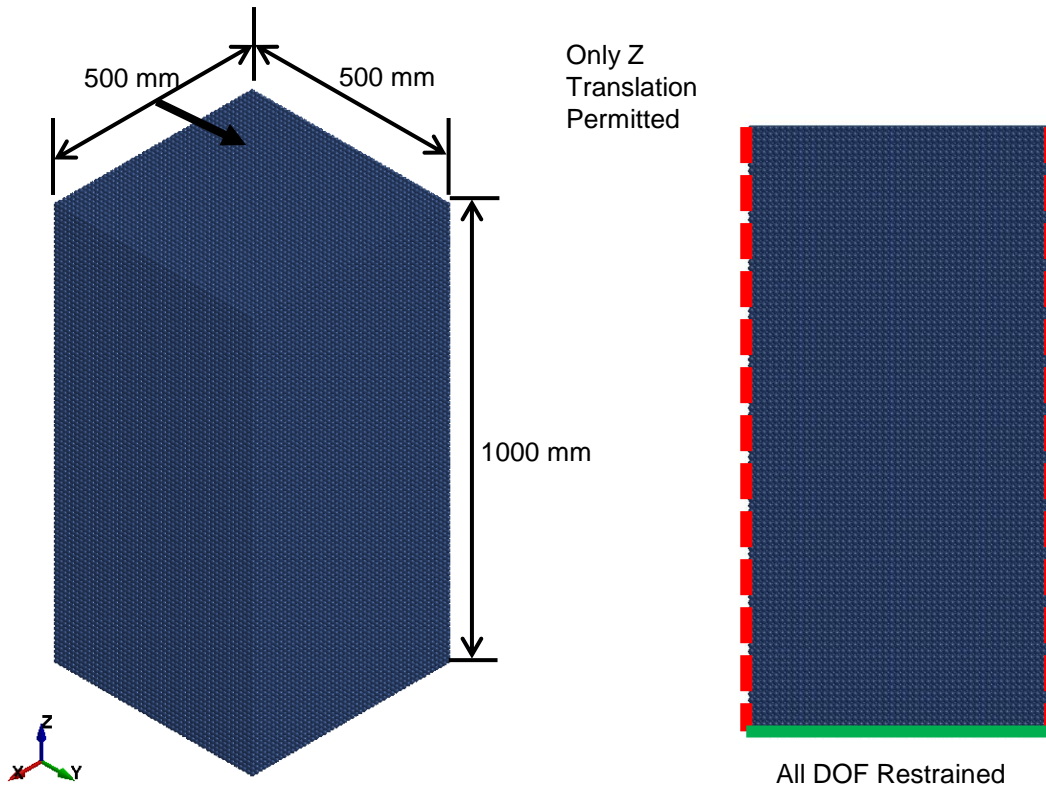
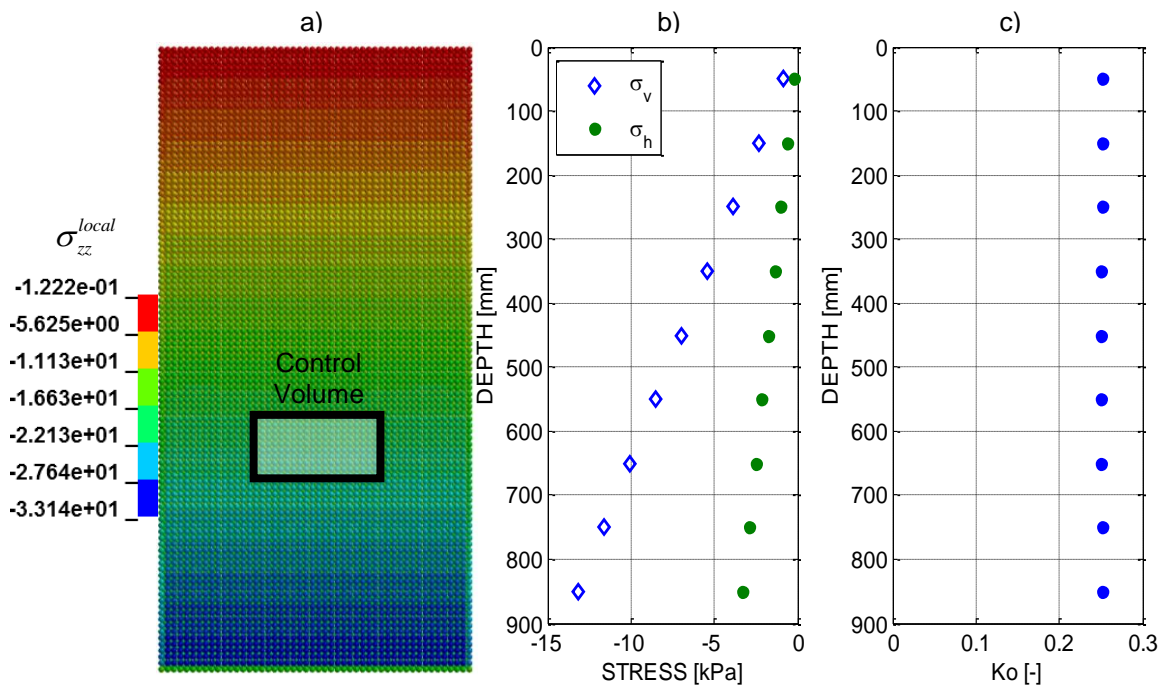*Fig.5:   Chamber test: a) Isometric View and Dimensions b) Gravitational Acceleration and Boundary Conditions.*

Fig.6:   Simple Cubic Binary Packing with FRIC = 0.30: a) Variation of σ_v b) Comparison of σ_v and σ_h c) Corresponding K_o.

These resulting K_o values are shown in Fig. 7. It can be seen for all geometric assemblies that increasing FRIC values correspond to decreases in K_o values. It can also be seen that the FCC packings develop the upper limit K_o values, whereas the Rhombic packings develop the lower limit values (for the range of parameters considered). K_o versus φ from direct shear test simulations are shown in Fig. 8. Comparing these results with Eqn. 1 (the solid line in Fig. 8), the idealized packings considered bound macroscopic-scale behaviors of coarse-grained soils (e.g., sand) as theorized by Jacky [3]. In consideration of the angularity and sphericity of sand particle shapes, Hendron [11] proposed:

$$K_o = \frac{1}{2} \left[\frac{1 + \frac{\sqrt{6}}{8} - 3\frac{\sqrt{6}}{8}\sin\varphi}{1 - \frac{\sqrt{6}}{8} + 3\frac{\sqrt{6}}{8}\sin\varphi} \right] \tag{7}$$

Eqn. 7 seems to provide a good bounded solution of K_o for numerically simulating macroscopic-scale shear behaviors of sands (using FCC packing assemblies of elastic spherical discrete elements with a uniform radius).
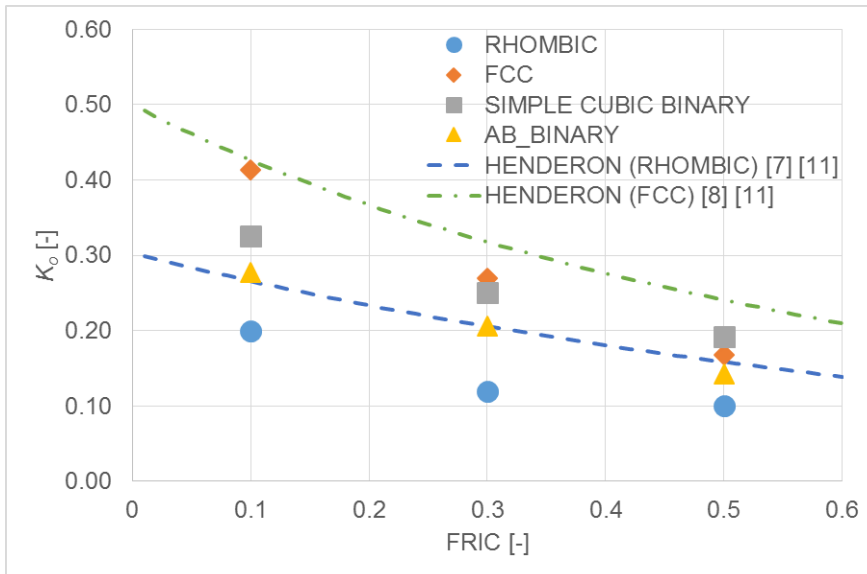

Fig.7: K_o *versus FRIC: Eqns. 2, 3, 4, and 7 are combined to determine* K_o *as a function of FRIC for the FCC and Rhombic packings*

5 Summary

This paper presents an analysis of volume-averaged stress states simulated over various geometric packing assemblies. A parametric study using direct shear test simulations is conducted to quantify the angle of internal friction (φ) for several types of packing. The φ values obtained from the direct shear test simulations indicate that geometric interlocking of the idealized assemblies impacts the numerical simulation of in-situ conditions. It is, thus, possible that the physical interlocking phenomenon at granule-scales can be simulated for idealized assemblies of discrete spherical elements with diameters that are relatively much larger than, in turn, the mean diameters of sand particle-size distributions. Numerical simulation results illustrate that predictions of φ values using the rhombic and FCC packings are much greater than those observed in laboratory experiments on coarse-grained soils. As for the various geometric packings considered, K_o can vary with the size of the discrete elements, as well as the predetermined control volume used to calculate macroscopic stresses. The idealized packing assemblies can additionally be used to chracterize the bounds of K_o

and φ for granular soils in in-situ conditions. This is particularly feasible when granular assemblies are simulated with consideration of spatial distribuitons (patterned or random) and other microscopic scale variations (e.g., shape and size distributions of granules).
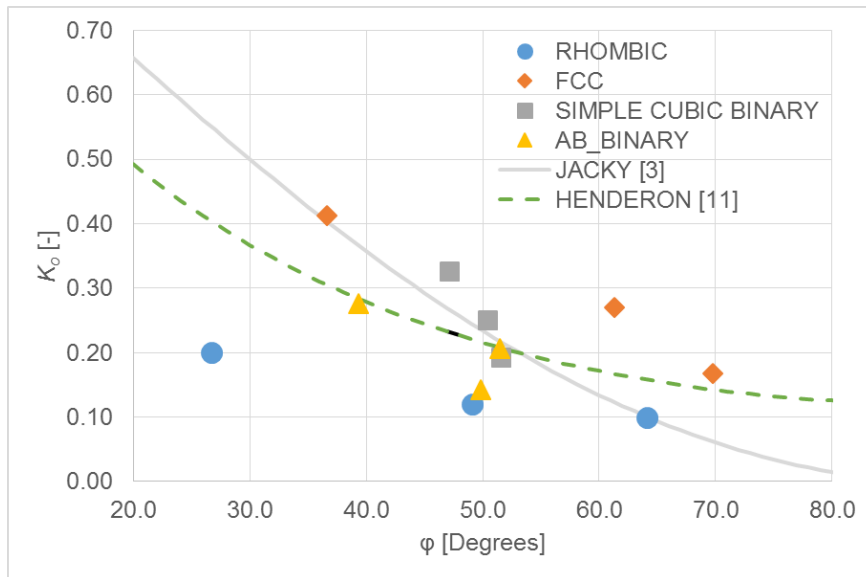

Fig.8: K_o *versus* φ .

6 Literature

[1]   Livermore Software Technology Corporation (LSTC): *LS-DYNA Keyword User's Manual Vol. I*, (2015), Livermore, California, USA.

[2]   Mitchell, J. K., & Soga, K. (1976). *Fundamentals of soil behavior* (p. 422). New York: Wiley.

[3]   Jaky, J. (1944). The coefficient of earth pressure at rest. *Journal of the Society of Hungarian Architects and Engineers*, *78*(22), 355-358.

[4]   Karajan, N., Zhidong, H., Ten, H., and Wang, J.: Interaction Possibilities of Bonded and Loose Particles in LS-DYNA®, (2013), *9th European LS-DYNA Conference.*

[5]   Cil, M. B., & Alshibli, K. A. (2014). 3D analysis of kinematic behavior of granular materials in triaxial testing using DEM with flexible membrane boundary. *Acta Geotechnica*, *9*(2), 287-298.

[6]   O'Sullivan, C., Bray, J. D., & Riemer, M. (2004). Examination of the response of regularly packed specimens of spherical particles using physical tests and discrete element simulations. *Journal of engineering mechanics*, *130*(10), 1140-1150.

[7]   Rowe, P. W. (1962, October). The stress-dilatancy relation for static equilibrium of an assembly of particles in contact. In *Proceedings of the Royal Society of London A: Mathematical, Physical and Engineering Sciences* (Vol. 269, No. 1339, pp. 500-527). The Royal Society.

[8]   Thornton, C. (1979). The conditions for failure of a face-centered cubic array of uniform rigid spheres. *Géotechnique*, *29*(4), 441-459.

[9]   O'Sullivan, C., Cui, L., & Bray, J. D. (2004). Three-dimensional discrete element simulations of direct shear tests. *Numerical Modeling in Micromechanics via Particle Methods*, 373-382.

[10]   Oda, M., & Iwashita, K. (1999). An Introduction mechanics of granular materials. AA BALKEMA, (1), 1-5.

[11]   Hendron Jr, A. J. (1963). *The Behavior of Sand in one Dimensional Compression*. Thesis submitted to the Univ. Of illinois at Urbana-Champaign for partial fulfillment of the requirements of Doctor of Philosophy.